Journal of Macromolecular Science, Part A
Publication details, including instructions for authors and subscription information:
http://www.informaworld.com/smpp/title~content=t713597274

Sorption Behavior of Permeants in the Polyurethane-Based Pervaporation Membranes Studied by DSC

Aleksandra Wolińska-Grabczyk[a]; Andrzej Jankowski[a]
[a] Institute of Coal Chemistry Polish Academy of Sciences, Gliwice, Poland

To cite this Article Wolińska-Grabczyk, Aleksandra and Jankowski, Andrzej(2005) 'Sorption Behavior of Permeants in the Polyurethane-Based Pervaporation Membranes Studied by DSC', Journal of Macromolecular Science, Part A, 42: 2, 157 — 173
To link to this Article: DOI: 10.1081/MA-200046972
URL: http://dx.doi.org/10.1081/MA-200046972

Journal of Macromolecular Science®Part A—Pure and Applied Chemistry, 42:157–173, 2005

ISSN 1060-1325 print/1520-5738 online
DOI: 10.1081/MA-200046972

Sorption Behavior of Permeants in the Polyurethane-Based Pervaporation Membranes Studied by DSC

ALEKSANDRA WOLIŃSKA-GRABCZYK
AND ANDRZEJ JANKOWSKI

Institute of Coal Chemistry Polish Academy of Sciences, Gliwice, Poland

Differential scanning calorimetry (DSC) was used to study sorption behavior of various liquid permeants in the pervaporation membranes formed of homologous series of polyether-, polyester-, and polydiene-based polyurethane elastomers. It has been found that there are three major types of liquid permeant within the membrane: (1) non-crystallizable liquid, (2) crystallizable-bound liquid, and (3) crystallizable-bulk liquid. The kind and number of these forms and their relative contribution appear to be a characteristic feature of a particular system and depend on the specific interactions between permeant and membrane material and between permeant molecules themselves. For weak polymer-permeant interactions compared to those concerning permeant, crystallizable-bulk liquid (3) has only been detected within the membrane. For moderate polymer/permeant interactions, represented by the sorption equilibrium values falling around 30%, the permeant in two different forms, (1) and (3), of various composition has been found to exist. For strong polymer/permeant interactions, all types of permeant have been observed including a form (2) classified as crystallizable-bound liquid. This type of liquid permeant, showing complex melting endotherm of significantly depressed T_m values, has been identified for the first time for permeants without hydrogen-bonding ability. The observed phenomena are considered as general behavior of membranes under pervaporation conditions and are expected to have an effect upon permeation.

Keywords polyurethane, sorption, pervaporation membrane, differential scanning calorimetry, permeant

Introduction

Contrary to the permanent gases for which the transport through dense polymer films is independent of pressure at a given temperature, the permeation behavior of condensable vapors and liquids strongly depends on the relative strengths of the interactions between the permeant molecules and the polymer, and between the permeant molecules themselves. In the extreme, a strong affinity of permeant towards membrane may lead to swelling or even dissolution of the membrane. On the other hand, strong negative interactions like ionic repulsion can prevent the permeant entering the membrane phase.

Received June 2004, Accepted June 2004
Address correspondence to Aleksandra Wolińska-Grabczyk, Institute of Coal Chemistry Polish Academy of Sciences, Sowińskiego 5, 44-121, Gliwice, Poland. E-mail: grabczyk@karboch.gliwice.pl

Depending on the magnitude and nature of the interaction forces, the permeant molecules may become immobilized at sites created by the polymer groups, or at pre-existing micro-voids or related structures. When cohesive forces between permeant molecules are greater then attractive forces between permeant and polymer, the permeant tend to cluster within the polymer, decreasing its mobility. Since the partitioning of the permeant between the free solution and the membrane phase, as well as its transport through the membrane phase are both influenced by strength and nature of these interactions, it is a topic of interest to obtain more knowledge on the behavior of the permeant molecules within the membrane.

One of the methods to study the state of liquid permeant in polymer membrane is differential scanning calorimetry (DSC). There are a number of studies on the states of water in various hydrophilic polymers,[1–4] or in polymers grafted with hydrophilic monomers.[5,6] It has been reported that three distinct behaviors of the sorbed water may be identified in those polymers. One is the lack of any first-order transition peak in the temperature range from $-123^{\circ}C$ to $27^{\circ}C$ below a certain critical water content, then the appearance of a multi-peak melting endotherm and a crystallization exotherm at $T < 0^{\circ}C$ for a higher water content. Finally, the presence of a melting endotherm at $T = 0^{\circ}C$, identical to that of bulk water, as the amount of the sorbed water further increases. These observations enabled three types of sorbed water to be differentiated: non-freezable bound water, freezable bound water, and free water.

The state of organic liquids in polymers received less attention, however it has been expected that organic liquid with high affinity towards a polymer can exhibit similar behavior. There are few studies on alcohol[2,7–9] and cyclohexane[10] sorbed in poly(dimethylsiloxane) (PDMS) showing that the investigated liquids can indeed be presented in the bound state, as well as in the bulk state in the polymer. The more comprehensive study concerning the behavior of various liquids, classified as "poor" solvents and "good" solvents, has been presented recently,[11] however, these investigations were also performed for PDMS, the same polymer studied by other authors.

The objective of the presented work was to investigate the state of liquid permeant in a polymeric membrane regarding both the structure of a polymer and the kind of liquid. The homologues series of polyurethane elastomers with modified soft segments, along with various liquids, have been used for these studies. These materials belong to a broad family of polyurethanes synthesized by us which have already been subject to extensive morphology analysis using small-angle X-ray scattering,[12,13] or atomic force microscopy[14] as well as to the investigations of their transport properties using the pervaporation method.[15–17] The systems chosen in this work comprise a wide range of polymer-solvent and solvent-solvent interactions resulting from the different nature and composition of the components. This should allow for a deeper knowledge about the behavior of a permeant in the membrane and their mutual interactions and to help defining factors, which influence the permeation properties of the polymers involved.

Experimental

Materials

Polyurethanes (PU) used in these studies were synthesized in a DMF solution in the reaction of equimolar amounts of 2,4-tolylene diisocyanate (TDI, Aldrich) with a macrodiol (or macrodiamine). Poly(oxytetramethylene) diol (PTMO, $M_n = 2000$, BASF), poly(oxypropylene) diol (PPO, $M_n = 2000$, Aldrich), poly(oxyethylene) diol (PEO, $M_n = 1000$, Aldrich),

poly(monoethylene adipate) diol (PEA, $M_n = 2000$, Alfa Systems), polybutadiene diol (BD, $M_n = 1200$, Aldrich) and poly(butadiene-co-acrylonitrile) diamine (BAN, $M_n = 570$, Aldrich) were applied. The details of the polyurethane synthesis have been described elsewhere.[16,17] The synthesized PUs were determined to have the relative molar masses (M_n), in the range of 35,000–55,000 compared with polystyrene standards, with molar mass distribution values close to 2, as expected for conventional condensation polymerization.

The PU films for the DSC studies were obtained in a similar way as the PU-based pervaporation membranes, by pouring the 15 wt% solution of a given PU in DMF onto a glass plate, and by evaporating the solvent at 60°C for 3 days. The analytical grade solvents were used in the swelling experiments.

Measurements

DSC measurements were performed on a Rheometric Plus differential scanning calorimeter, after previous calibration with benzene for melting temperature and enthalpy. Each sample was cooled down to −150°C and held at that temperature for 2 min. Then, the DSC measurements were carried out up to 30°C at a heating rate of 10°/min. Melting or crystallization temperatures were taken as the endotherm or exotherm maximum peak values, and the corresponding enthalpies were measured by integration of the peak areas. Polyurethane films of thickness of about 300 μm were immersed in the liquid studied at 25°C for a time required to reach the equilibrium saturation. After equilibrium was attained, the films were taken from the liquid, blotted with a filter paper to remove the liquid from the film surface, cut into 5 mm discs using a special knife, and put into aluminium sample pans. Then, the DSC measurements started, which were renewed for every sample at various time intervals for a period of time necessary for desorption of liquid from the sample, i.e., until no peak was observed in the DSC thermograms. Measurements were repeated several times with freshly swollen sample each time to receive the data comprising the wide range of swelling degrees. After the DSC measurements, the pans were opened and polymers were dried in vacuum at 60°C. The liquid content in the sample at a particular swelling degree was determined by subtracting the weight of a dry polymer from the weight of a swollen one.

The amount of non-crystallizable solvent in the membrane was determined by plotting enthalpic heats of melting for a given solvent as a function of its total content in the membrane and by extrapolating the resulting linear relationship to $\Delta H = 0$. The intercept with the solvent content axis is equal to the amount of the non-crystallizable solvent (see Fig. 1).

Results and Discussion

The PU elastomers studied in this work were selected based on the chemical nature of the macrodiol used in the PU synthesis. This kind of structural variations allowed the wide modulation of the PU hydrophobicity, starting from hydrophilic PEO-based PU to a hydrophobic BD-based one. The differences in chemical nature between particular PUs are illustrated by the solubility parameter values listed in Table 3 for some of the polymers corresponding to the polyurethane soft segments. In accordance with these data, various solubilities of a particular solvent in the PUs studied have been observed. Thus, the sorption equilibrium values received from the isothermal sorption experiments have been used as a measure of the respective affinity of the membrane materials towards

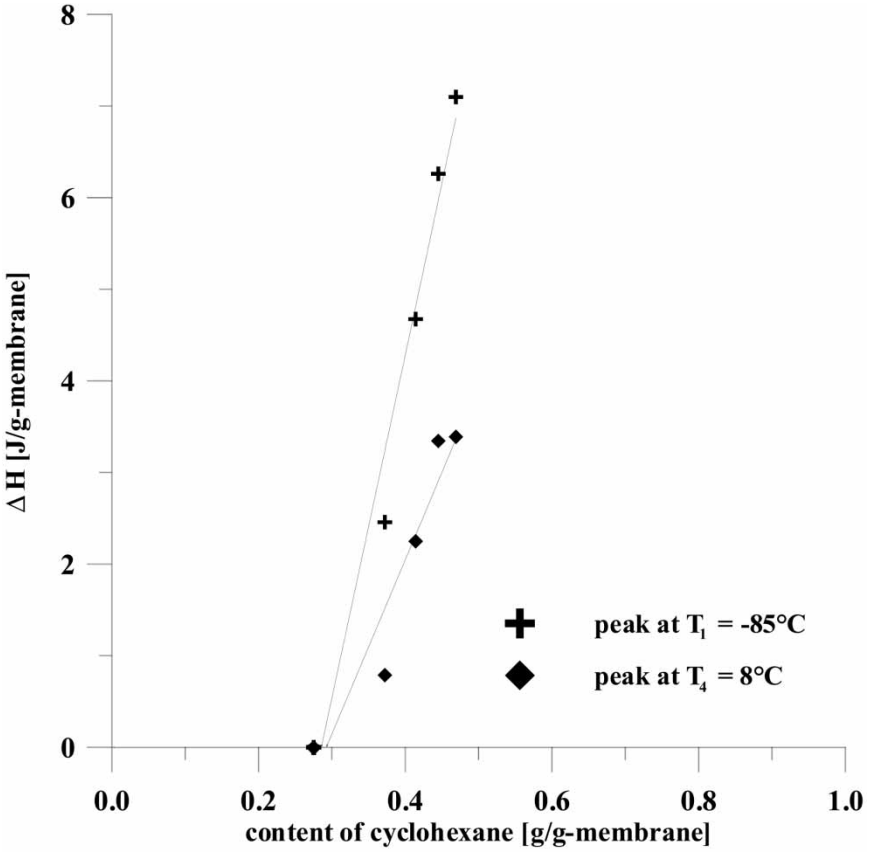

Figure 1. Variations of the transition enthalpies with cyclohexane content for polybutadiene-based PU.

different liquid permeants. To minimize the effect of the hard segment domains on the properties of the investigated PUs, the polymers were synthesized without a chain extender keeping the weight fraction of the hard segments as low as possible.

Water in Polyurethanes

Three polyether-based PUs with different hydrophobicity, from hydrophilic PU-PEO to hydrophobic PU-PTMO, were used in these studies. As is generally observed for all PUs studied in this work, besides the glass transition of the soft segments of the dry PUs, the DSC thermograms reveal only the characteristic features of the solvent sorbed. The results of water sorption and its melting behavior in the PUs tested are given in Table 1.

An example of the melting endotherms of water in PU-PEO at different degrees of swelling is shown in Fig. 2.

The melting endotherms of the sorbed water seem to be similar to that of pure water for all three PUs, however the melting point depression can be observed which follows the set of increasing sorption equilibrium values determined for those polymers. As is displayed by the data in Table 1, the shift of the endotherm maximum is of a opposite direction than could be expected based on the amount of solvent in the membrane samples. Along with the shift of

Table 1
Phase transition temperatures and enthalpies of water in polyurethanes at various degrees of swelling

Sample	Equilibrium swelling [wt%]	Swelling degree [wt%]	Crystallization		Melting		Content of non-crystallizable water [wt%]
			T_c [°C]	ΔH_c[a] [J/g]	T_1 [°C]	ΔH_1[a] [J/g]	
PU-PEO	85.6	83	—	—	0.4	64.8	
		51	−24.2	3.4	−1.5	30.1	
		38	−26.6	8.9	−3.6	16.3	27
		31	−26.3	3.5	−5.4	4.4	
PU-PPO	27.9	15			1.5	24.2	
		10			0.8	14.3	
		6			0.2	9.9	1.5
		3			−1.0	2.4	
PU-	PTMO	9.3	4			1.0	6.9
	0						
	2			0.7	1.2		
Pure					0.3_{onset}/ 2.6	207	

[a][J/g-membrane].

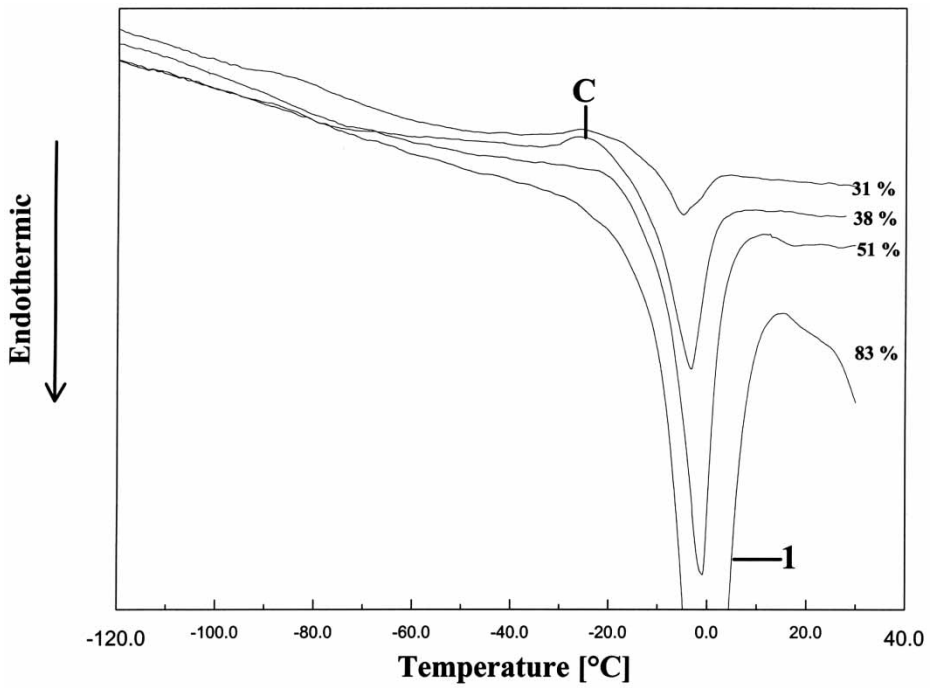

Figure 2. DSC heating curves of poly(ethylene oxide)-based PU/water system at different swelling degrees (wt%).

the melting point towards lower temperatures, there is also an increase in the amount of non-crystallizable water in those membranes. From the data obtained, it may be concluded that almost all water in the PU-based membranes of higher hydrophobicity (PU-PTMO, PU-PPO) exists in a form of bulk water. In PU-PEO with the highest affinity towards water, two states of water can be distinguished depending on its total amount sorbed. At low water content, up to 27%, the lack of any peaks in the DSC thermograms indicates that the sorbed water is in the non-crystallizable state. At equilibrium saturation, only one peak corresponding to the melting of bulk water is observed (see Fig. 2). However, at intermediate water content, a small crystallization peak, followed by a melting peak can be detected at the heating run. This melting peak has also been identified as melting of the normal ice of free water, which shows a depression of its transition temperature due to the perturbing action of the polymer chains. The disturbing effect of the macromolecules is found to be greater, the smaller the water content in membrane. This effect can also account for the crystal formation during the heating step, which involves water molecules not having enough time to crystallize during the cooling process.

Cyclohexane in Polyurethanes

The state of cyclohexane in structurally different polyurethanes was studied for the selected polydiene-based PUs (PU-BD and PU-BAN) and polyether-based PUs (PU-PPO and PU-PTMO).

As can be seen from Table 2, the differences in chemical nature of the macrodiols chosen as the PU soft segment precursors are closely related to the observed differences in the affinity of the resulting polymers towards cyclohexane, displayed by the sorption equilibrium values. The DSC thermograms illustrating the transition behavior of cyclohexane in this set of polymers are shown in Figs. 3 and 4. The values of melting temperatures and enthalpies at various degrees of swelling are given in Table 2. In the thermogram of pure cyclohexane two endotherms are observed, at $-84^{\circ}C$ ($-87^{\circ}C$, onset) for solid-solid transition, and at $8.8^{\circ}C$ ($7.2^{\circ}C$, onset) for solid-liquid transition. The similar pattern can be observed for melting of cyclohexane sorbed in PU-BD and PU-PPO (see the representative DSC thermograms in Fig. 3).

No melting point depression other than that resulting from the decreasing amount of cyclohexane for lower swelling degrees, and no additional peaks, neither endotherm nor exotherm, have been detected in the DSC thermograms of those polymers. On the other hand, a significantly high amount of cyclohexane has appeared to be in a form unable to crystallize. This part constitutes even 74% of the total amount of cyclohexane in PU-PPO at equilibrium saturation and about 40% of cyclohexane in PU-BD. In the thermograms of cyclohexane in PU-PTMO and PU-BAN, an additional two endotherms have been observed within the temperature range from $-84^{\circ}C$ to $8.8^{\circ}C$, between the temperatures corresponding to both transitions of bulk cyclohexane (see the example in Fig. 4).

The experimental data for PU-PTMO, relating the enthalpic heat of the transition initially observed at $-26.6^{\circ}C$ to the cyclohexane content, gives the straight line intersecting the cyclohexane content axis at the same point obtained by extrapolating the data of the bulk cyclohexane transition at $-84^{\circ}C$ to $\Delta H = 0$. The enthalpic heat values of other extra transitions observed for PU-PTMO or PU-BAN were too low to allow any meaningful results to be obtained. However, the same values of the amount of non-crystallizable cyclohexane obtained as a result of the two independent extrapolations enable the assumption to be made, that the new endotherms detected in the DSC thermograms originate from a transition of cyclohexane alone. The data in Table 2 show that as the cyclohexane

Table 2
Phase transition temperatures and enthalpies of cyclohexane in polyurethanes at various degrees of swelling

Sample	Equilibrium swelling [wt%]	Swelling degree [wt%]	Solid-solid transition		Melting						Content of non-crystallizable cyclohexane [wt%]
			T_1 [°C]	ΔH^a [J/]	T_2 [°C]	ΔH^a [J/]	T_3 [°C]	$\Delta H_3{}^a$ [J/g]	T_4 [°C]	ΔH^a [J/]	
PU-PPO	34.0	31	—	0.6					8.5	0.3	25
			85.5								
		45	—	0.8	—	6.7	2.0	1.2	8.4	—	
			84.5		26.6						
		40	—	0.6	−28	4.8	0.8	1.0	8.4	—	
			84.5								
PU-PTMO	64.8	35	—	0.2	—	3.0	1.2	1.0	8.4	—	22
			84.5		29.5						
		27	—	—	—	1.2	2.1	0.6	—	—	
					31.2						
		23	—	—	—	0.4	6.5	0.7	—	—	
					41.7						
		19	—	—	—	—	8.5	0.5	—	—	
PU-BD	66.5	47	−85	7.1					8.1	3.4	
		41	−85	4.7					7.5	2.2	29
		37	−85	2.5					7.3	0.8	
		47	—	1.5	—	1.1	0.4	1.2			
			84.5		36.5						
PU-BAN	47	43	—	0.8	—.	1.0	0.4	0.6			34
			84.5		38.5						
		38	—	0.4	—	0.3	0.2	0.3			
			84.5		37.5						
		36	—	0.1	—	—	−1.4	0.2			
			84.5								
Pure cyclohexane		$-87_{onset}/-$		72.8					$7.2_{onset}/8.8$	26.2	

[a] [J/g-membrane].

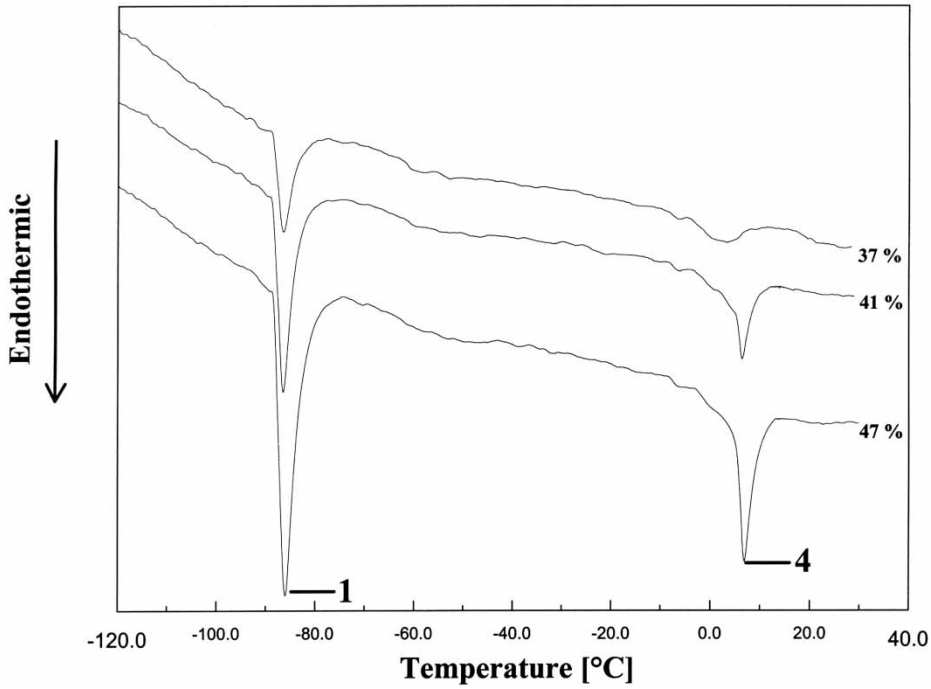

Figure 3. DSC heating curves of poly(butadiene)-based pu/cyclohexane system at different swelling degrees (wt%).

content in PU decreases, the position of both endotherms generally shifts towards lower temperatures. This shift is especially marked for PU-PTMO, for which the heats of the new transitions are higher than those corresponding to the transitions of bulk cyclohexane.

From the results presented, it appears that three kinds of cyclohexane can be distinguished in PUs: (1) non-crystallizable cyclohexane, which shows no endothermic peak in the temperature range from 30°C to −150°C, (2) crystallizable-bound cyclohexane with two different melting points, well below 0°C and round 0°C, (3) crystallizable-bulk cyclohexane showing solid-to solid transition at −84.5°C and melting at about 8°C. For the PUs investigated, the amount of non-crystallizable cyclohexane in all membranes is found to be remarkably high. Its dependence on the polyurethane structure, however, seems to be less pronounced than is observed for the amount of cyclohexane at equilibrium saturation. The bulk cyclohexane, the concentration of which depends on the kind of PU, has also been detected in each of the PUs studied. The third kind of cyclohexane, which has been found in two of the PUs investigated, PU-PTMO and PU-BAN, corresponds to the form of crystallizable-bound solvent, not reported in the literature so far. Moreover, it seems to be the major state of cyclohexane in PU-PTMO. The two endotherms in the low temperature region, which characterize the melting behavior of the new type of cyclohexane, can be explained as being attributed to the melting of crystals, the structure of which are different from each other and from that of the pure solvent due to the disturbing effects of the polymer chains. Surprisingly, this type of bound solvent has not been detected in PU-BD showing the highest affinity towards cyclohexane, as it comes from the sorption equilibrium value, as well as from the smallest difference in the solubility parameters between BD and cyclohexane.

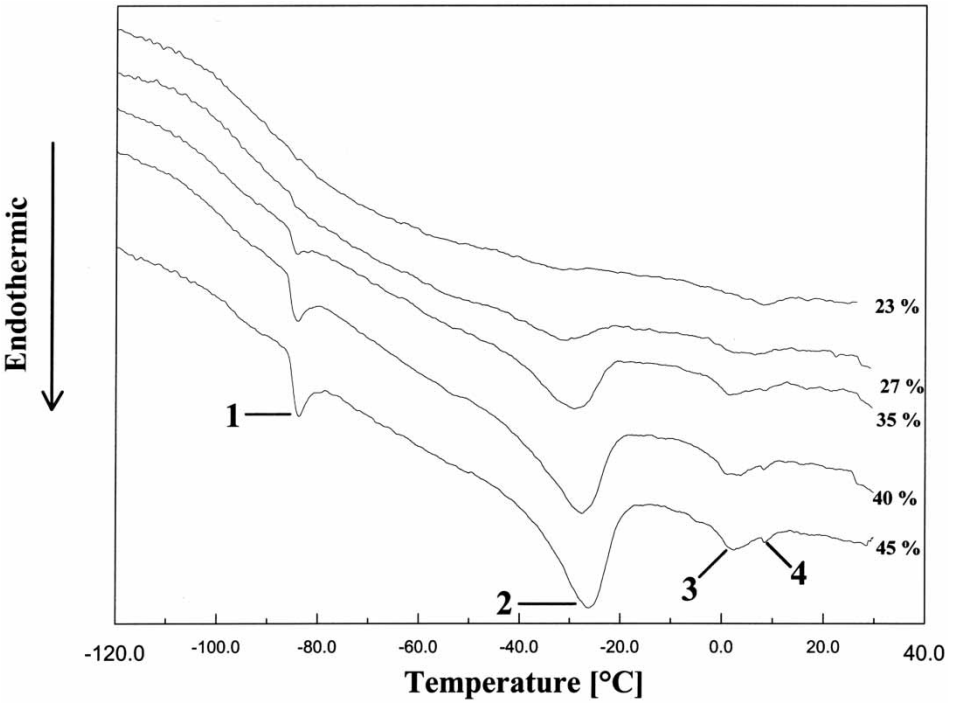

Figure 4. DSC heating curves of poly(tetramethylene oxide)-based PU/cyclohexane system at different swelling degrees (wt%).

Benzene in Polyurethanes

A broad range of PUs varying in the kind of the soft segments, like polyether-, polyester-, and polydiene-based PUs has been used to study the state of benzene in those structurally different membranes. The DSC thermograms for a series of PU/benzene systems are presented in Figs. 5–9, and the values of the transition temperatures and enthalpies for benzene in various PUs in Table 3.

Solubility parameters of polymers and solvents $[(\text{cal}/\text{cm}^3)^{1/2}]$: PEO $\delta = 9{,}9$; PPO $\delta = 9.1$; PTMO $\delta = 8.7$; BD $\delta = 8.2$; BAN $\delta = 9{,}0$; water $\delta = 23.4$; cyclohexane $\delta = 8.2$; benzene $\delta = 9.2$.

The typical set of DSC scans of PU at different degrees of swelling clearly shows complex melting endotherms and crystallization exotherms over a broad temperature range of about 80°C. The only exception is PU-PEO for which the DSC curves show a single and rather sharp peak similar to that representing the melting of bulk benzene (Fig. 5).

This peak, designated as peak 3, can also be identified in the multi-peak endotherms found for other PUs. The T_m determined from the position of this peak is initially around 7°C for all PUs and decreases with decreasing benzene content, approaching the values from the temperature range of -0.5°C to -13.4°C, depending on the PU structure. For PU-PEO and PU-PEA, showing the lowest sorption capacity at equilibrium saturation, no significant changes in the T_m value with the swelling degree have been observed. On the other hand, the highest shift in the peak position, of the order of 20°C, has been noted for PU-BAN, the polymer exhibiting the highest affinity towards benzene demonstrated by the highest equilibrium swelling value.

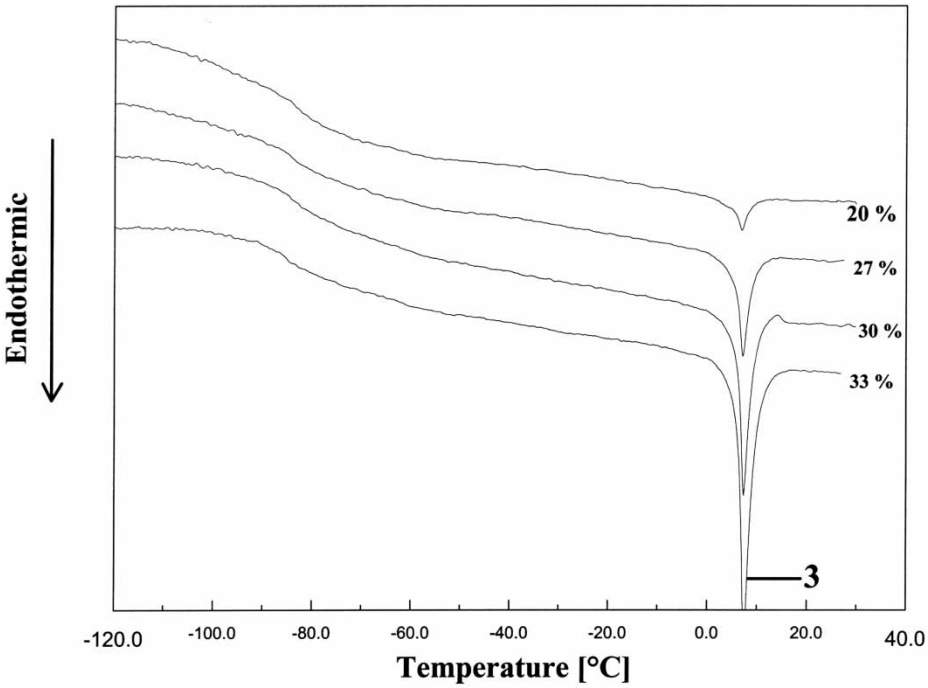

Figure 5. DSC heating curves of poly(ethylene oxide)-based PU/benzene system at different swelling degrees (wt%).

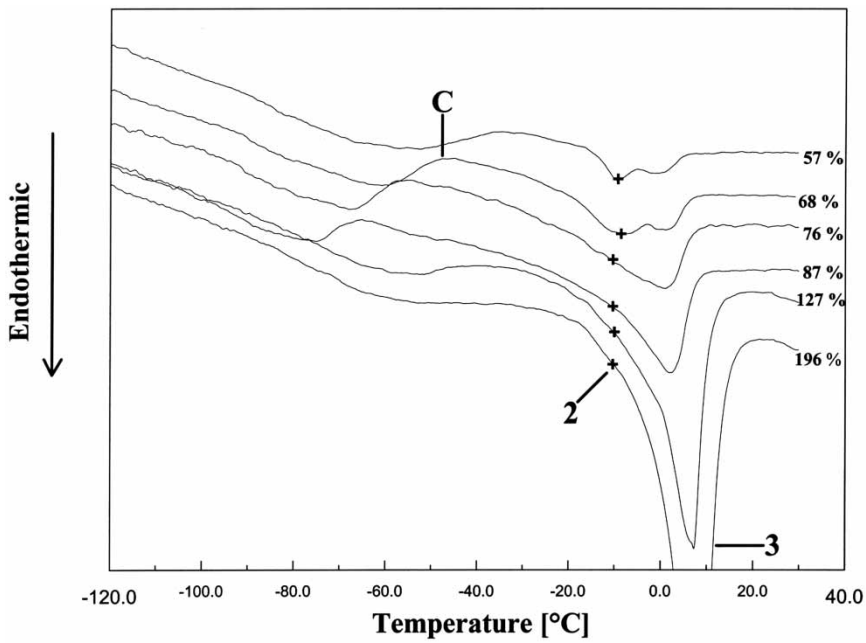

Figure 6. DSC heating curves of poly(propylene oxide)-based PU/benzene system at different swelling degrees (wt%).

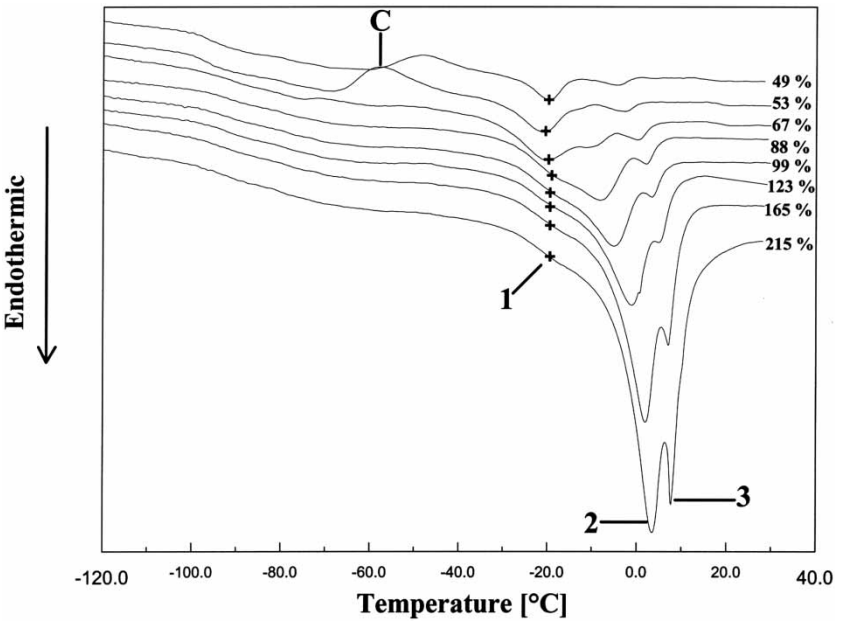

Figure 7. DSC heating curves of poly(tetramethylene oxide)-based PU/benzene system at different swelling degrees (wt%).

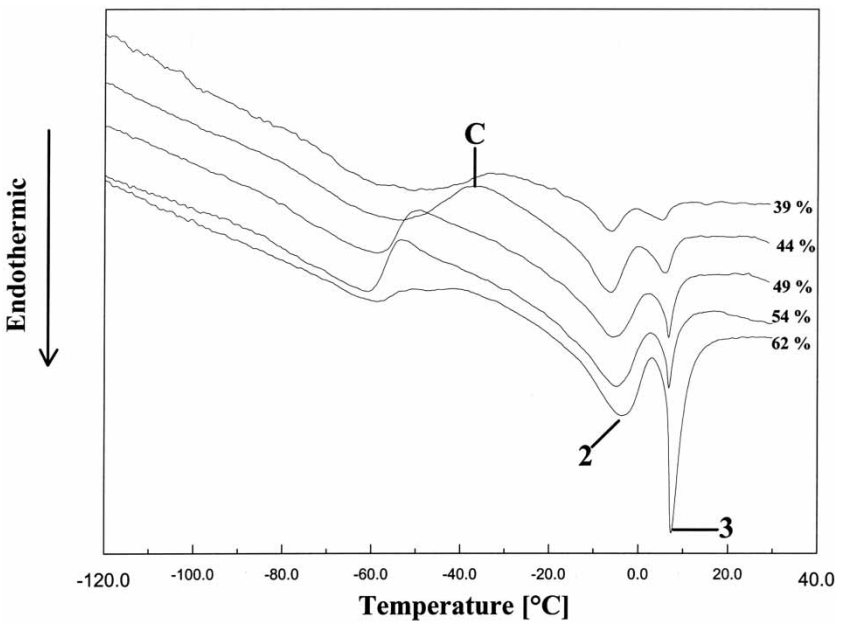

Figure 8. DSC heating curves of poly(monoethylene adipate)-based PU/benzene system at different swelling degrees (wt%).

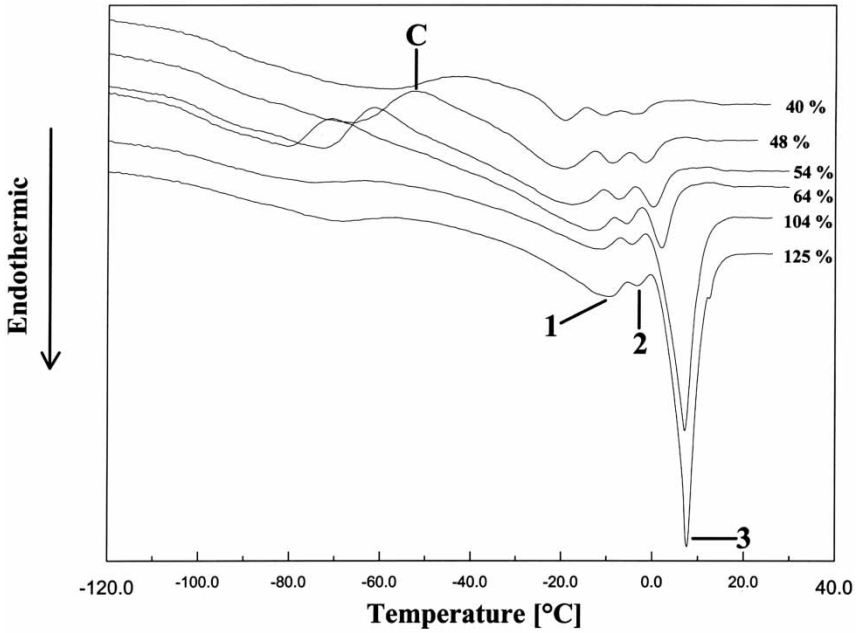

Figure 9. DSC heating curves of poly(butadiene)-based PU/benzene system at different swelling degrees (wt%).

In the DSC thermograms of the PUs investigated, except of PU-PEO with the lowest sorption equilibrium value, another peak (denoted as peak 2) showing lower T_m can be detected in the broad multi-peak endotherms. For PU-PPO and PU-BAN, exhibiting high affinity towards benzene, this peak is initially seen as a shoulder on the high intensity endotherm at 8°C (see example in Fig. 6).

As the benzene content decreases, however, this shoulder changes to a separate peak observed in the DSC curves of other PUs (Figs. 7–9). The position of this second endothermic peak depends on the kind of PU, even at high swelling degrees, and shifts to the lower temperature side with decreasing benzene content in a similar manner as peak 1. Another distinct behavior may also be identified for the group of PUs discussed above. This refers to the crystallization of super-cooled benzene which can be observed below a certain swelling degree. The crystallization exotherm, designated as C, appears in the temperature range from −71°C to −54°C depending on the kind of PU, and is shifted towards higher temperatures up to −34°C for lower swelling degrees.

For PU-PTMO and PU-BD with intermediate sorption equilibrium values, another transition can be distinguished in the complex melting endotherm. This is observed as a separate peak, designated as peak 1, for PU-BD (see Fig. 9) and for PU-PTMO at low swelling degrees, or as a shoulder for PU-PTMO with a higher benzene content (Fig. 7). Previously, the position of this endothermic peak shifts towards lower temperatures with decreasing benzene content.

The values of the total enthalpy corresponding to the multi-peak melting endotherms reported in Table 3, are found to decrease with a decrease in benzene content in the membrane. The comparison of these values with the respective crystallization enthalpies of the super-cooled benzene shows that the difference between both data sets observed for high swelling degrees is strongly reduced as the benzene content decreases. Taken into

Table 3
Phase transition temperature and entalphies of benzene in polyurethanes at different degrees of swelling

Sample	Equilibrium swellig [wt%]	Swellig degree [wt%]	Crystallizaton		Melting					Content of non-crystallizable benzene [wt%]
			T_c [°C]	ΔH_c[a] [J/g]	T_1 [°C]	T_2 [°C]	T_3 [°C]	ΔH_3[a] [J/g]	ΔH_{13}[a] [J/g]	
PU-PEO	33.1	33					7.1	10.1		
		30					7.0	7.0		15
		27					6.8	4.4		
		20					6.6	2.1		
PU-PPO	254.4	196	—	—		sh	7.9		56.0	
		127	—	—		sh	6.8		42.1	
		87	−65.8	6.7		sh	1.7		28.5	35
		76	−57.7	11.0		sh	0.6		19.6	
		68	−47.8	10.2		−8.9	−0.5		13.6	
		57	−36.7	7.3		−9.4	−0.5		7.0	
PU-PTMO	216.4	215	—	—	sh	3.2	7.2		75.4	
		165	—	—	sh	2.0	6.7		68.3	
		123	—	—	sh	−0.7	4.4		64.1	
		99	—	—	sh	−5.3	2.6		50.0	27
		88	—	—	sh	−8.6	1.5		43.3	
		67	—	—	−20	−11.0	−0.6		38.0	
		53	−57.9	13.6	−21.7	sh	−4.2		20.7	
		49	−48.7	8.1	−19.8	—	−4.7		12.7	

(*continued*)

Table 3
Continued

Sample	Equilibrium swellig [wt%]	Swellig degree [wt%]	Crystallizaton		Melting					Content of non-crystallizable benzene [wt%]
			T_c [°C]	ΔH_c[a] [J/g]	T_1 [°C]	T_2 [°C]	T_3 [°C]	ΔH_3[a] [J/g]	ΔH_{13}[a] [J/g]	
PU-PEA	67.4	62	—	—		−3.8	6.9		27.6	
		54	−53.8	12.4		−5.1	6.5		19.6	
		49	−49.6	11.1		−5.2	6.5		16.2	33
		44	−38.6	9.9		−6.1	5.4		9.5	
		39	−33.8	4.1		−6.0	4.8		4.7	
PU-BD	150.8	134	—	—	−12.1	−4.1	7.6		49.4	
		125	—	—	−10.3	−3.1	7.2		42.2	
		104	—	—	−11.0	−4.2	6.7		34.3	
		64	−71.1	11.1	−13.2	−5.2	6.7		31.5	27
		54	−61.8	16.3	−17.8	−7.0	−0.2		26.9	
		48	−53.4	14.5	−19.9	−8.7	−1.4		19.3	
		40	−46.2	7.7	−19.1	−10.4	−4.2		11.7	
PU-BAN	639	270	—	—		sh	7.9		67.9	
		162	—	—		sh	4.8		48.0	
		110	—	—		sh	0		37.8	23
		88	—	—		sh	−2.3		32.1	
		62	−67.7	1.9		−25.1	−9.3		20.2	
		50	−60.4	11.1		−29.9	−13.4		17.3	
Pure benzene						6.3_{onset}/8.8		105.9		

[a][J/g-membrane].

account the measurement accuracy, this difference becomes barely significant for most of the PUs at low swelling degrees suggest that the part of crystallizable benzene left in the membrane is able to crystallize only upon heating as a super-cooled solvent. The changes in the melting enthalpies plotted against the benzene content in the membrane give straight lines, which do not pass through the origin for all PUs investigated (see example in Fig. 1). This indicates that there is also a part of benzene in the membranes which is in a form of non-crystallizable bound solvent. The amount of non-crystallizable benzene, determined by extrapolating the data of the melting endotherm to $\Delta H = 0$, is in the range of 15–35% with the smallest values found for PU-PEO exhibiting the lowest affinity towards benzene.

From these results, it is found that there are three major forms in which benzene, like cyclohexane, can be present in the PU-based membranes, namely: (1) non-crystallisable benzene, (2) crystallizable-bound benzene, and (3) crystallizable-bulk benzene. Generally, all these forms have been identified alongside each of the PU studied. The different forms of crystallizable benzene may be characterized by their progressively decreasing T_m, starting from that corresponding to bulk solvent. The T_m values become further shifted towards lower temperatures as the benzene content in the membrane decreases. This behavior can reflect a sorption process where every part of benzene has its structure resulting from the interactions with its own microenvironments. The similar behavior has also been discovered for PU/cyclohexane systems with high affinity towards cyclohexane. Moreover, the results show that variety of solvent structures may be related to the strength of the attraction forces between permeant and membrane material. However, if such interactions are extremely high causing excessive swelling of the membrane, as it is observed for PU-BAN/benzene and PU-PPO/benzene systems, the diversity of the structures has been found to become limited. The strong attraction forces, which become more important for the lower degrees of swelling, can also account for the lower T_m values of the bound structures, as well as for the melting point depression with decreasing solvent content, or for the crystallization of super-cooled solvent during the heating run. At the extreme, this can lead to a situation where the structures formed by solvent molecules at the low solvent content are unable to crystallize or have their phase-transition temperatures extremely low, well below the temperature range available with the DSC equipment used. Such behavior can also be described as a single phase system resulting from the perfectly random mixing of the two components in the binary system composed of polymer and solvent molecules.

Conclusions

The behavior of liquid permeants in the pervaporation membranes studied may be described by the variability of forms in which the permeant can exist within the membrane. It has been found that generally three major types of permeant can be distinguished, which are different in structure and physicochemical properties: non-crystallizable liquid, crystallizable-bound liquid, and crystallizable-bulk liquid. The kind and number of the forms present and their relative amount appear to be a characteristic feature of a given system that can be related to the strength of the attraction forces between permeant and membrane material and between permeant molecules themselves.

For weak polymer/permeant interactions compared to those between permeant molecules, such as in the PU-PTMO/water system, the permeant in a form of crystallizable-bulk liquid has only been identified, similarly as in the PDMS/water system.[9]

For moderate polymer/permeant interactions, represented by the sorption equilibrium values falling around 30 wt%, the permeant in two different forms, as non-crystallizable liquid and crystallizable-bulk liquid, has been found to exist. The contribution of both forms is seen to change significantly from one system to another and appears to be associated with the differences in the relative strength of the particular attraction forces. The values of 5 wt% and 74 wt%, representing the contribution of a non-crystallizable form in the total amount of permeant in the PU-PPO/water and PU-PPO/cyclohexane systems respectively, can illustrate such behavior. Analogous observations on the existence of permeate in a state of non-crystallizable liquid and crystallizable-bulk liquid have been made for the systems composed of the PDMS membrane and lower alcohols such as 2-propanol[9] and ethanol,[8] as well as for the PDMS/cyclohexane system.[10]

For strong polyurethane/permeant interactions, characterized by the sorption equilibrium values exceeding 50 wt%, another type of permeant has been observed. This can be either in a form of crystallizable-bulk liquid with its melting point markedly depressed, such as for the PU-PEO/water system, or in a form of multiple structures with significantly distinct and strongly depressed T_m values. The melting point depression, comparable with that registered for the PU-PEO/water system, and the presence of different bulk states at high solvent contents, have been observed for permeants named as good solvents in PDMS.[12] However, the second type of crystallizable permeant discovered in several PU/permeant systems, significantly different from the bulk form, has not been described in the literature yet. This form can be classified as crystallizable-bound permeant based on the resemblance to one of the types of sorbed water in hydrophilic polymers.[3,6] The partial crystallization of permeant during the heating run can also be observed in the systems with strong mutual interactions. As stated previously, the number of the permeant structures and their relative contribution are thought to depend on the relative strength of different forces of attraction between correspondent sites in the membrane and permeant.

The results demonstrated here lead to the general conclusion that the diversity of the permeant structures, which can be present alongside within the membrane, is not only confined to the systems with the strong hydrogen-bonding ability, but can be regarded as a characteristic feature of the membrane under pervaporation conditions. Thus, the observed phenomena should be considered in the evaluation of the efficiency of the pervaporation membrane. For instance, the results show that the kind, number and relative contribution of the permeant forms should change from the surface of the membrane being in contact with the liquid feed to the permeant side of the membrane. At the swollen side of the membrane, the existence of all permeant forms attributable to a given system can be expected. In contrast, at the permeant side of membrane, the presence of non-crystallizable permeant can be assumed. It is reasonable to assume, therefore, that the distribution of the permeant forms, according to the concentration profile, occurs within the membrane, as it can be deduced from the experimental data concerning the effect of the membrane swelling degree on the state of permeant. Considering that both the concentration of the individual form and its mobility can affect the transport process, further work is required to establish the relationship between those parameters and their contribution to the transport mechanism.

Acknowledgments

We are grateful to the State Committee for Scientific Research of Poland, Grant No. 3T09B07719, for financial support of this research.

References

1. Higuchi, J.; Komiyama, J.; Iijima, T. The states of water in gel cellophane membranes. Polym. Bull. **1984**, *11*, 203–208.
2. Nguyen, T.; Favre, E.; Ping, Z.H.; Neel, J. Clustering of solvents in membranes and its influence on membrane transport properties. J. Membr. Sci. **1996**, *113*, 137–150.
3. Higuchi, A.; Iijima, T. DSC investigation of the states of water in poly(vinyl alcohol-co-itaconic acid). Polymer **1985**, *26*, 1833–1837.
4. Ping, Z.H.; Nguyen, Q.T.; Chen, S.M.; Zhou, J.Q.; Ding, Y.D. States of water in different hydrophilic polymers–DSC and FTIR studies. Polymer **2001**, *42*, 8461–8467.
5. Takigami, S.; Kimura, T.; Nakamura, Y. The state of water in nylon-6 membranes grafted with hydrophilic monomers: 2. Water in acrylic acid, acrylamide and p-styrenesulphonic acid grafted nylon-6 membranes. Polymer **1993**, *34*, 604–609.
6. Chan, K.; Hirotsu, T.; Hatakeyama, T. DSC studies on bound water in polypropylene films plasma-grafted with 2-hydroxyethyl acrylate and acrylic acid or methacrylic acid. Eur. Polym. J. **1992**, *28*, 1021–1025.
7. Yoshikawa, M.; Matsuura, T. A calorimetric study of various alcohols in a poly(dimethylosiloxane) membrane. Polymer **1992**, *33*, 4656–4658.
8. Yoshikawa, M.; Handa, Y.P.; Cooney, D.; Matsuura, T. Anomalous physicochemical properties of ethanol in a polymeric membrane. Macromol. Chem., Rapid Comm. **1990**, *11*, 387–391.
9. Yoshikawa, M.; Matsuura, T.; Cooney, D. Studies on the state of permeant in the membrane ant its effect on pervaporation phenomena. J. Appl. Polym. Sci. **1991**, *42*, 1417–1421.
10. Yoshikawa, M.; Cooney, D.; Matsuura, T. Anomalous physico-chemical behavior of cyclohexane in a poly(dimethylosiloxane) membrane. Polym. Comm. **1991**, *32*, 555–557.
11. Yang, H.; Nguyen, Q.T.; Ding, Y.D.; Long, Y.C.; Ping, Z. Investigation of poly(dimethyl siloxane) (PDMS)-solvent interactions by DSC. J. Membr. Sci. **2000**, *164*, 37–43.
12. Grigoriew, H.; Wolińska-Grabczyk, A.; Chmielewski, A.G.; Amenitch, H.; Bernstorff, S. SAXS study of the influence of ethanol on the microstructure of polyurethane-based membrane. J. Membr. Sci. **2000**, *170*, 275–279.
13. Grigoriew, H.; Wolińska-Grabczyk, A.; Plusa, M.; Bernstorff, S. Kinetics of the structural changes in polyurethanes saturated with benzene during the desorption process. J. Mat. Sci. Lett. **2002**, *21*, 1179–1182.
14. (a) Wolińska-Grabczyk, A.; Żak, J.; Muszyński, J.; Jankowski, A. Surface morphology of the polyurethane-based pervaporation membranes studied by Atomic Force Microscopy: 1. Effect of the polyurethane molecular structure. J. Macromol. Sci., PAC **2003**, *A40*, 225–237; (b) Wolińska-Grabczyk, A.; Żak, J.; Muszyński, J.; Jankowski, A. Surface morphology of the polyurethane-based pervaporation membranes studied by Atomic Force Microscopy: 2. Structure-transport properties behavior. J. Macromol. Sci., PAC **2003**, *A40*, 335–344.
15. Wolińska-Grabczyk, A. Optimization of transport properties of the polyurethane-based pervaporation membranes by a polymer molecular structure design. Macromol. Symp. **2002**, *188*, 117–130.
16. Muszyński, J.; Wolińska-Grabczyk, A.; Penczek, P. Synthesis, characterization and pervaporation properties of segmented poly(urethane-urea)s. J. Appl. Polym. Sci. **1999**, *71*, 1615–1625.
17. Wolińska-Grabczyk, A. Relationships between permeation properties of the polyurethane-based pervaporation membranes and their structure studied by a spin probe method. Polymer **2004**, *in press*.